DOI: 10.1002/cphc.200900696

The Role of Ion Pairs in the Second-Order NLO Response of 4-X-1-Methylpiridinium Salts**

Francesca Tessore,*[a] Elena Cariati,[a] Franco Cariati,[a] Dominique Roberto,[a] Renato Ugo,[a]
Patrizia Mussini,[b] Cristiano Zuccaccia,[c] and Alceo Macchioni[c]

A series of 4-X-1-methylpyridinium cationic nonlinear optical (NLO) chromophores (X = (*E*)-CH=CHC$_6$H$_5$; (*E*)-CH=CHC$_6$H$_4$-4′-C(CH$_3$)$_3$; (*E*)-CH=CHC$_6$H$_4$-4′-N(CH$_3$)$_2$; (*E*)-CH=CHC$_6$H$_4$-4′-N(C$_4$H$_9$)$_2$; (*E,E*)-(CH=CH)$_2$C$_6$H$_4$-4′-N(CH$_3$)$_2$) with various organic ($CF_3SO_3^-$, *p*-$CH_3C_6H_4SO_3^-$), inorganic (I^-, ClO_4^-, SCN^-, $[Hg_2I_6]^{2-}$) and organometallic (*cis*-$[Ir(CO)_2I_2]^-$) counter anions are studied with the aim of investigating the role of ion pairing and of ionic dissociation or aggregation of ion pairs in controlling their second-order NLO response in anhydrous chloroform solution. The combined use of electronic absorption spectra, conductimetric measurements and pulsed field gradient spin echo (PGSE) NMR experiments show that the second-order NLO response, investigated by the electric-field-induced second harmonic generation (EFISH) technique, of the salts of the cationic NLO chromophores strongly depends upon the nature of the counter anion and concentration. The ion pairs are the major species at concentration around 10^{-3} M, and their dipole moments were determined. Generally, below 5×10^{-4} M, ion pairs start to dissociate into ions with parallel increase of the second-order NLO response, due to the increased concentration of purely cationic NLO chromophores with improved NLO response. At concentration higher than 10^{-3} M, some multipolar aggregates, probably of H type, are formed, with parallel slight decrease of the second-order NLO response. Ion pairing is dependent upon the nature of the counter anion and on the electronic structure of the cationic NLO chromophore. It is very strong for the thiocyanate anion in particular and, albeit to a lesser extent, for the sulfonated anions. The latter show increased tendency to self-aggregate.

1. Introduction

The structural features of organic and organometallic molecules necessary to produce significant second-order nonlinear optical (NLO) properties are well known; for instance, in the last two decades many different architectures of the so-called one-dimensional (1D) push–pull NLO chromophores have been investigated.[1]

In 1D push–pull cationic NLO chromophores the positive charge lowers the energy of intramolecular charge transfer (ICT), and thus leads to an increase in the second-order NLO response. A detailed investigation on the second-order NLO responses of a series of *N*-methyl and *N*-aryl pyridinium salts was done by Coe et al,[2] who showed that their ICT is characterized by a significant increase in dipole moment upon excitation from the ground to the excited state ($\Delta\mu_{eg}$), and therefore they are the origin of a considerable static quadratic hyperpolarizability β_0. The second-order NLO response was measured by the hyper Rayleigh scattering (HRS) technique and by an indirect method involving the Stark effect, with acetonitrile as solvent or in butyronitrile glasses at 77 K and with PF_6^- as counter anion in order to avoid ion pairing as much as possible.

Using solvents of lower dielectric constant or counter anions of higher polarizability could introduce a relevant role of ion pairing in controlling the second-order NLO response of these cationic 1D push–pull NLO chromophores, since the nature of the counter anion may play a significant role in controlling the alignment of these cationic NLO chromophores in the crystalline structure[3,4] and also in self-assembled thin films[5] of some of their salts.

To investigate the role of ion pairing, we explored the effect of the nature of the counter anion on the second-order NLO response of various 4-X-1-Methylpyridinium salts (X = (*E*)-CH=CHC$_6$H$_5$ (**1**); (*E*)-CH=CHC$_6$H$_4$-4′-C(CH$_3$)$_3$ (**2**); (*E*)-CH=CHC$_6$H$_4$-4′-N(CH$_3$)$_2$ (**3**); (*E*)-CH=CHC$_6$H$_4$-4′-N(C$_4$H$_9$)$_2$ (**4**); (*E,E*)-(CH=CH)$_2$-C$_6$H$_4$-4′-N(CH$_3$)$_2$ (**5**); see Table 1) in a solvent of low dielectric con-

---

[a] *Dr. F. Tessore, Prof. E. Cariati, Prof. F. Cariati, Prof. D. Roberto, Prof. R. Ugo*
Dipartimento di Chimica Inorganica
Metallorganica e Analitica "Lamberto Malatesta"
dell'Università degli Studi di Milano
and Unità di Ricerca di Milano dell'INSTM
Via G. Venezian, 21-20133 Milano (Italy)
Fax: +39-02-50314405
E-mail: francesca.tessore@unimi.it

[b] *Prof. P. Mussini*
Dipartimento di Chimica Fisica ed Elettrochimica
dell'Università di Milano
Via C. Golgi, 19-20133 Milano (Italy)

[c] *Dr. C. Zuccaccia, Prof. A. Macchioni*
Dipartimento di Chimica
dell'Università di Perugia
Via Elce di Sotto, 8-06123 Perugia (Italy)

[**] *The Relevant Role of Ion Pairs and of their Dissociation and Aggregation in Chloroform Solution on the Second-Order Nonlinear Optical Response of Salts of Various 4-X-1-Methylpyridinium Chromophores: A Spectroscopic, EFISH, Conductimetric and PGSE NMR Investigation (EFISH: electric-field-induced second harmonic generation, PGSE: pulsed field gradient spin echo)*

Table 1. Salts of the 4-X-1-methylpyridinium NLO chromophores investigated herein.

			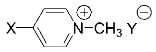		
X	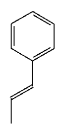	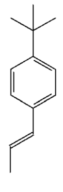	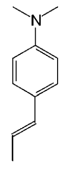	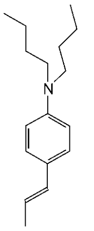	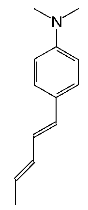
	1	**2**	**3**	**4**	**5**
Y⁻	I^-	I^-	I^-	$CF_3SO_3^-$ I^- ClO_4^- SCN^- pTS^{-}[a] $[Hg_2I_6]^{2-}$ [*cis*-$Ir(CO)_2I_2]^-$	I^-

[a] pTS^-: *p*-toluensulphonate

stant such as anhydrous $CHCl_3$. The effect of organic ($CF_3SO_3^-$, *p*-$CH_3C_6H_4SO_3^-$), inorganic (I^-, ClO_4^-, SCN^-, $[Hg_2I_6]^{2-}$) and organometallic (*cis*-$[Ir(CO)_2I_2]^-$) counter anions of quite different polarizability and size was also investigated.

The second-order NLO response was measured by means of the electric-field-induced second harmonic generation (EFISH) technique,[6] usually considered off-limits for ionic species. However, a recent paper[7] showed that this technique could be applied for determination of the second-order NLO response of the iodide of a 1-methylpyridinium chromophore in $CHCl_3$, a solvent of low dielectric constant which should favour ion pairs. The use of the EFISH technique, specially suitable for 1D NLO chromophores, instead of HRS[8] can avoid possible overestimation of the value of the quadratic hyperpolarizability due to multiphoton fluorescence[9] when a non-resonant 1.907 μm incident wavelength or a femtosecond laser is not used.[2]

Previously, some of us reported[10,11] on the strong dependence upon concentration in $CHCl_3$ solution of the product $\mu\beta_{1.91}$ measured by the EFISH technique ($\beta_{1.91}$ is, for the sake of simplicity, the EFISH quadratic hyperpolarizability at an incident wavelength of 1.907 μm) of Zn^{II} complexes with push–pull stilbazole ligands such as **c** and **d** (see Figure 1) and a sulfonated anion such as trifluoromethanesulfonate (triflate) as ancillary ligand. At concentrations below 10^{-4} M, the value of $\mu\beta_{1.91}$ remarkably increases with decreasing concentration and reaches very large values. Given the low nucleophilicity of the triflate anion, this behaviour was explained by solvolysis of the triflate ligand to produce first a kind of ion pair, which then dissociates by further dilution to finally generate a cationic Zn^{II} complex, characterized by an enhanced second-order NLO response due to the presence of a positive charge. Careful investigations of the electrical conductivity of anhydrous $CHCl_3$ solutions of these sulfonated complexes were in agreement with progressive ionic dissociation.[10,11]

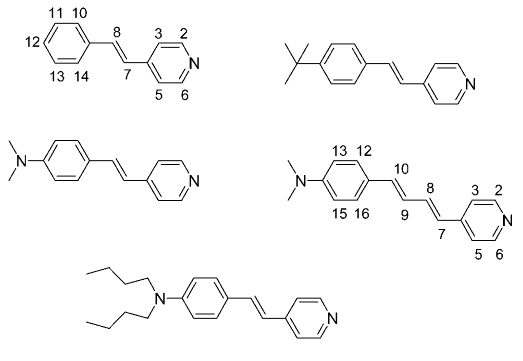

Figure 1. Stilbazolic precursors of the cationic NLO chromophores investigated herein.

Herein we investigate whether some salts of the 1D cationic NLO chromophores presented in Table 1 show in anhydrous $CHCl_3$ solution a second-order NLO response which is strongly dependent on the nature of the counter anion and on concentration, as expected for progressive dissociation of ion pairs by dilution or for their aggregation by increasing concentration. The EFISH investigation is also supplemented by a careful conductivity investigation, which to our knowledge is the first comprehensive case study of the conductimetric behaviour of organic salts in a low-polarity solvent such as anhydrous $CHCl_3$, and by pulsed field gradient spin echo (PGSE) NMR experiments, which have proven to be a useful tool for evaluating the degree of aggregation of molecular species in solution.[12]

2. Results and Discussion

2.1. Synthesis of Salts of Pyridinium 1D Second-Order NLO Chromophores with Various Counter Anions

The various salts of the 1D pyridinium second-order NLO chromophores investigated herein are reported in Table 1. While the iodides of **3** and **4** are commercially available, the iodides of **1**, **2** and **5** were synthesised by reaction of the corresponding stilbazolic precursor (Figure 1) with an excess of iodomethane in toluene or CH_2Cl_2 solution at room temperature for 2 h. The iodides were obtained in satisfactory yield (60–75%) by crystallization of the crude products from CH_3CN/Et_2O (**1**) or CH_2Cl_2/*n*-hexane (**2** and **5**). The triflate salt of **4** was synthesized by reaction of the commercially available iodide with a stoichiometric amount of $AgCF_3SO_3$ in CH_3CN solution at room temperature, followed by crystallization of the crude product from CH_2Cl_2/*n*-hexane (88% yield). In a similar way, reaction in

CH_3CN solution of the iodide of **4** with the appropriate silver salt [Ag(4-$CH_3C_6H_4SO_3$), $AgClO_4$, AgSCN] in a stoichiometric ratio at room temperature for 2 h, followed by crystallization of the crude product from CH_3CN or CH_2Cl_2/*n*-hexane, afforded the corresponding salts of **4** in satisfactory yield (60–80 %).

The salt of **4** with $[Hg_2I_6]^{2-}$ was obtained in EtOH solution by reaction of mercury(II) iodide with two equivalents of the iodide of **4** at room temperature. The crude product was crystallized from CH_2Cl_2/*n*-hexane (47 % yield). Finally, the salt of **4** with *cis*-$[Ir(CO)_2I_2]^-$ was synthesized by a slight modification of that reported in the literature.[13] The black polymeric species $[Ir(CO)_2Cl]_n$, obtained by reaction of $[\{Ir(COT)_2Cl\}_2]$ (COT = cyclooctene) with CO, was treated with an excess of KI, affording K{*cis*-$[Ir(CO)_2I_2]$}, which was finally added as an aqueous suspension to a stirred solution of the iodide of **4** in CH_2Cl_2. The final product was obtained in 40 % yield by appropriate work-up of the CH_2Cl_2 layer (see the Experimental Section).

2.2. Spectroscopic Investigations and Measurements of Dipole Moments

2.2.1. ^1H NMR Spectra

In the ^1H NMR spectra in $CDCl_3$ (see Experimental Section) of the iodide salts, the signals of hydrogen atoms in α position to the pyridine nitrogen atom at around 8 ppm are shifted to lower fields compared to the corresponding stilbazolic precursor (for example, $\Delta\delta = 0.87$ ppm for **1**; $\Delta\delta = 0.83$ ppm for **2**; $\Delta\delta = 0.47$ ppm for **5**), as expected for enhanced electron-withdrawing character of the positively charged nitrogen atom of the pyridine ring.

For the various salts of **4** (see Table 1), the signals of the hydrogen atoms in α position to the pyridinic nitrogen atom are at only slightly higher fields compared to those of the iodide ($\Delta\delta$ is in the range 0.02–0.4 ppm), varying from 8.33 ppm for the salt with *cis*-$[Ir(CO)_2I_2]^-$ to 8.71 ppm for the salt with 4-$CH_3C_6H_4SO_3^-$.

In all the salts of **1**–**5**, the coupling constant of the protons of the double bond is 15-16 Hz, as expected for the *E* geometry around the C–C double bond.

2.2.2. Dipole Moments and Electronic Absorption Spectra

Dipole moments μ of the various salts (Tables 2 and 3) were measured in anhydrous $CHCl_3$ solution by the Guggenheim method[14] at concentration around 10^{-3} M. The dipole moments of ion pairs of some quaternary salts in a series of different solvents, including $CHCl_3$, in a range of concentrations around 10^{-3} M were carefully investigated by Grunwald and co-workers.[15] They reported that, in this range of concentrations, electrolytic dissociation in $CHCl_3$ is relatively small. Therefore, the correction of the linear plots of dielectric constant versus concentration due to ionic dissociation is negligible, in accordance with the very good linear plots of capacitance versus concentration that we have experimentally obtained (see Experimental Section). Interestingly, the Guggenheim method seems to be appropriate for determination of the

Table 2. Electronic absorption spectra, dipole moments, EFISH $\mu\beta_{1.91}$ values and molar conductivities Λ of various 4-X-1-methylpiridinium iodides, measured in anhydrous $CHCl_3$ solution.

Cation	λ_{max} [nm]	μ [D]	EFISH $\mu\beta_{1.91}$ [10^{-48} esu]	Λ [Ω^{-1} cm^2 mol^{-1}]
1	357	9.1	800[a]	0.22[a]
			300[b]	0.12[b]
			170[c] (15.8[e])	0.10[c]
2	377	10.1	810[a]	0.33[a]
			600[b]	0.17[b]
			205[c] (16.2[e])	0.12[c]
3	503[d]	14.4	1700[a]	0.63[a]
			1000[b]	0.34[b]
			1000[c] (46.3[e])	0.34[c]
4	519	15.8	1900[a]	
			1400[b]	0.63[a]
			1090[c] (45[e])	0.33[b]
			1040[f]	0.28[c]
			925[g]	
5	532	n.d.	1860[a]	0.55[a]
			1600[b]	0.27[b]
			1450[c]	0.22[c]

[a] Concentration 10^{-4} M. [b] Concentration 5×10^{-4} M. [c] Concentration 10^{-3} M. [d] Emission of **3** was studied in $CHCl_3$ at different concentrations. $\lambda_{em} = 577$ nm at 5.5×10^{-6} M and $\lambda_{em} = 603$ nm at 5.5×10^{-4} M. [e] β_0 ($\times10^{-30}$ esu) calculated by the two-level model from the $\beta_{1.91}$ value at 10^{-3} M.[36] [f] Concentration 5×10^{-3} M. [g] Concentration 10^{-2} M.

Table 3. Electronic absorption spectra, dipole moments, EFISH $\mu\beta_{1.91}$ and molar conductivity Λ of various salts of (*E*)-4-(4′-dibutylaminostyryl)-1-methylpiridinium, measured in $CHCl_3$ solution.

Anion	λ_{max} [nm]	μ [D]	EFISH $\mu\beta_{1.91}$ [10^{-48} esu]	Λ [Ω^{-1} cm^2 mol^{-1}]
$CF_3SO_3^-$	515	8.5	1150[a]	0.58[a]
			710[b]	0.34[b]
			225[c] (17.7[e])	0.28[c]
I^-	519	15.8	1900[a]	0.63[a]
			1400[b]	0.33[b]
			1090[c] (45[e])	0.28[c]
			1040[f]	
			925[g]	
ClO_4^-	520	7.3	1950[a]	0.61[a]
			1200[b]	0.33[b]
			250[c] (22.1[e])	0.27[c]
SCN^-	515	13.0	1800[a]	0.79[a]
			1800[b]	0.39[b]
			1790[c] (90.6[e])	0.27[c]
pTS^{-}[d]	509	13.2	1150[a]	0.14[a]
			780[b]	0.10[b]
			690[c] (34.5[e])	0.10[c]
$[Hg_2I_6]^{2-}$	532	n.d.	6050[a]	2.37[a]
			4200[b]	0.92[b]
			3850[c]	0.64[c]
cis-$[Ir(CO)_2I_2]^-$	523	19.6	2020[a]	1.10[a]
			1250[b]	0.60[b]
			1180[c] (38.8[e])	0.43[c]

[a] Concentration 10^{-4} M. [b] Concentration 5×10^{-4} M. [c] Concentration 10^{-3} M. [d] pTS$^-$ = *p*-toluenesulfonate. [e] β_0 ($\times10^{-30}$ esu) calculated by the two-level model from the $\beta_{1.91}$ value at 10^{-3} M.[36] [f] Concentration 5×10^{-3} M. [g] Concentration 10^{-2} M.

dipole moment of ion pairs of these pyridinium salts (Table 1), although Grunwald and co-workers usually measured the dipole moment of ion pairs of some other quaternary salts by applying the more sophisticated Onsager–Kirkwood method.[16]

The dipole moments of the ion pairs are, as expected, quite high. For example, the dipole moment of the iodide of **2** is 10.1 D (Table 2), while that of the neutral compound obtained by coordination of the related stilbazole **b** to the $[Os_3(CO)_{11}]$ moiety was reported to be only 5.1 D.[17a] Accordingly, for the iodide of **3**, the dipole moment is 14.4 D (Table 2), while those of the neutral complexes of the corresponding stilbazole **c**, coordinated to *cis*-$[Ir(CO)_2Cl]$, *cis*-$[Ir(COT)_2Cl]$, *cis*-$[Rh(CO)_2Cl]$, $[Rh(COD)Cl]$ and *fac*-$[Os(CO)_3Cl_2]$ were reported to be significantly lower (6.0, 8.1, 7.0, 6.7, and 7.4 D respectively).[17b]

The dipole moments of salts of **4** with other counter anions are still quite high and dependent upon the nature of the counter anion. For instance, salts with relatively small anions of low polarizability such as $CF_3SO_3^-$ (8.5 D) and ClO_4^- (7.3 D) show the lowest values (Table 3).

The significant differences in the dipole moments in $CHCl_3$ solution of ion pairs of **4** with various counter anions can be partially attributed, according to Grunwald et al.,[15] to a change in the average interionic structure of the ion pairs, due to the different contributions to the total dipole moment of the various counter anions. This contribution is large for large counter anions like *cis*-$[Ir(CO)_2I_2]^-$ (19.6 D) and *p*-toluenesulfonate (13.2 D), as opposed to the smaller contribution of trifluoromethanesulfonate (8.5 D). Besides the additional contributions of the anion and cation to the dipole moment (μ) of the ion pair, μ could also depend on the average interionic distance, which explains, for instance, the increase in dipole moment in $CHCl_3$ compared to other solvents with negligible dipole contributions (e.g., anisole or chlorobenzene).[15] This effect may explain the unexpectedly large dipole moments of the iodides of **3** and **4** (14.4 and 15.8 D, respectively).

Electronic absorption spectra were recorded in $CHCl_3$ solution (Tables 2 and 3). For the iodides, the major absorption band is red-shifted in comparison with that of stilbazolic precursors **a**–**e**.[17] This shift depends upon the nature of the electronic transition associated with the absorption. For example, for the iodides of **1** and **2**, the absorption bands at 357 nm (3.47 eV) and 377 nm (3.29 eV), respectively, are red-shifted by only 0.55 and 0.13 eV, since these absorptions can be attributed to internal π–π^* transitions that are less affected by the quaternization process. On the contrary, in the absorption spectra of the iodides of NLO chromophores carrying the strongly electron donating dibutylamino or dimethylamino groups, such as **3** and **5**, the major absorption band at about 500–530 nm (2.48–2.34 eV), which involves charge transfer from the HOMO to the LUMO, the former of which is a π-bonding molecular orbital located primarily on the aminophenyl unit,[2b,18,19a] is quite strongly affected by the quaternization process, due to significant lowering of the π^* energy level of the acceptor pyridine ring. In accordance, the red shift of these absorptions is significant (0.85 and 0.8 eV for **3** and **5**, respectively).

Interestingly, for the various salts of **4**, the shift of the ICT band (Table 3) is dependent on the size and polarizability of the counter anion, as expected for ion pairing. For instance, the red shift when the counter anion is large, for example, $[Hg_2I_6]^{2-}$ or *cis*-$[Ir(CO)_2I_2]^-$, is higher (0.83–0.85 eV), respectively) than when the counter anion is of smaller size (around 0.77–0.80 eV). In fact, in the former case a higher positive charge on the nitrogen atom of the pyridine ring is expected, due to the increased average interionic distance in the structure of the ion pair.

Evidence for further aggregation of ion pairs is given when the electronic absorption spectra of the iodide of **3** are recorded at different concentrations in various solvents. In $CHCl_3$ (dielectric constant $\varepsilon = 4.8$, the lowest among those considered), the absorption maximum of the ICT shows a slight blue shift with increasing concentration only at concentrations above 10^{-3} M, while in CH_2Cl_2 ($\varepsilon = 8.9$) and 1,2-dichloroethane ($\varepsilon = 10.65$), already at lower concentrations (about 10^{-4} M), blue shifts of up to 0.07 and 0.04 eV, respectively, occur with increasing concentration.

This blue shift suggests that in solvents of low or medium permittivity such as $CHCl_3$, CH_2Cl_2 and 1,2-dichloroethane progressive formation of H aggregates of the ion pairs occurs.[20,21] These shifts are more significant in emission spectra.[21] For instance, significant red shift of the emission band related to the ICT of the iodide of **3** was observed with increasing concentration already in the range 10^{-6}–10^{-4} M (at 5.5×10^{-6} M, $\lambda_{em} = 577$ nm, while at 5.5×10^{-4} M, $\lambda_{em} = 603$ nm, with a shift of 0.09 eV).

2.3. EFISH Investigation of the Second-Order NLO Responses in $CHCl_3$ of Various Salts of 4-X-1-Methylpyridinium

The EFISH technique[6] was used to investigate the second-order NLO responses of the salts of NLO chromophores **1**–**5**. Measurements were carried out in anhydrous $CHCl_3$ at an incident wavelength of 1.907 μm (1.91 μm for the sake of simplicity), chosen to generate a second harmonic (at 955 nm) far enough from the major ICT absorption band typical of these NLO chromophores, and thus to minimize dispersive enhancement of the NLO response.[22] The experimental error is about 10%.

The $\mu\beta_{1.91}$ values were plotted versus concentration for the iodides of **1**–**5** (Figure 2A) and for the various salts of **4** (Figure 2B, where pTS^- denotes *p*-toluenesulfonate). In all cases, decreasing the concentration from 10^{-3} to 10^{-4} M increases the $\mu\beta_{1.91}$ value by a factor varying from 1.3-fold (for the iodide of **5**) to 7.8-fold (for the perchlorate of **4**). With increasing dilution a further strong increase of $\mu\beta_{1.91}$ occurs, but below a concentration of 10^{-4} M the EFISH signal-to-noise ratio becomes too low to obtain sufficiently reproducible quantitative $\mu\beta_{1.91}$ measurements. The only exception to this trend is the thiocyanate of **4**, which does not show an increase in $\mu\beta_{1.91}$ on dilution (Figure 2B).

For the iodide of **4** a $\mu\beta_{1.91}$ value of 840×10^{-48} esu, measured in $CHCl_3$ by the EFISH technique, was reported, but without details on concentration.[7] Such a value is similar to that of

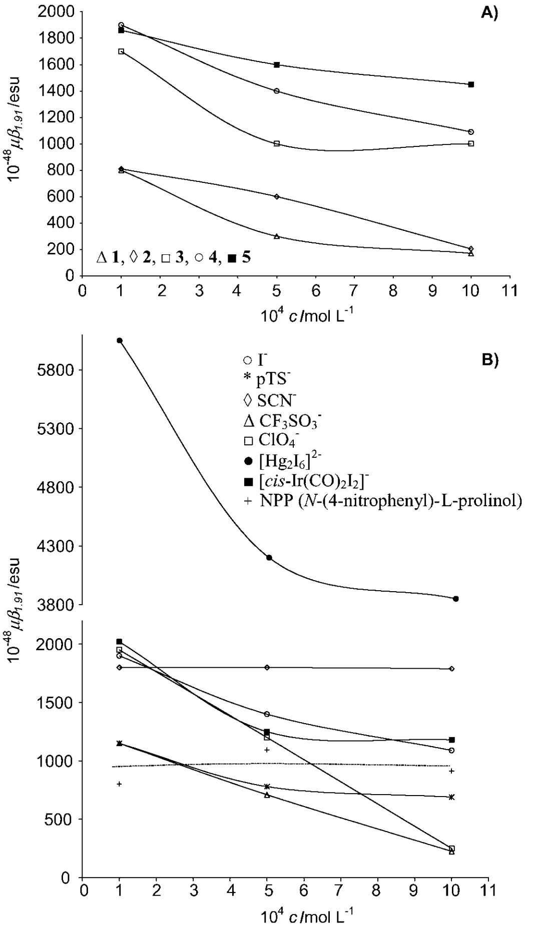

Figure 2. Plot of $\mu\beta_{1.91}$ versus molar concentration *c* of the iodides of **1**–**5** (A) and various salts of **4** (B).

1090×10^{-48} esu (Table 3) obtained by us at a concentration of 10^{-3} M, as is usually adopted for EFISH measurements.

The increase in $\mu\beta_{1.91}$ with decreasing concentration may be associated with increased ionic dissociation of ion pairs on dilution, to generate a higher concentration of weakly or even non-associated cationic NLO chromophores. These should be characterized by an increased second-order NLO response compared to the corresponding ion pair, due to the increased positive charge on the pyridine ring, which lowers the energy of the π^* orbitals.[10,11]

Figure 2A evidences that the EFISH data of the iodides of **1**–**5** can be divided into two groups: those with cationic NLO chromophores characterized by the absence of the ICT band, such as **1** and **2**, and those with cationic NLO chromophores having a significant ICT band, such as **3**, **4** and **5**. At each concentration, the $\mu\beta_{1.91}$ values of the first group (iodides of **1** and **2**) are considerably lower (5–7 times) than those of the second group (iodides of **3**, **4** and **5**), as expected for the lack of an ICT transition at lower energy.

Lengthening of the π-delocalised bridge between the donor and acceptor groups of the NLO chromophore increases[17b] the second-order NLO response, as reported for other NLO chromophores (at 5×10^{-4} M, the iodide of **5** shows a $\mu\beta_{1.91}$ value of 1600×10^{-48} esu, as opposed to 1000×10^{-48} esu for the iodide of **3**).

At the lowest concentration reliably investigated (10^{-4} M), the value of $\mu\beta_{1.91}$ reaches rather comparable values for the various iodides of the two groups (800×10^{-48} esu for **1** and 810×10^{-48} esu for **2** in the first group and 1700×10^{-48} esu for **3**, 1900×10^{-48} esu for **4** and 1860×10^{-48} esu for **5** in the second group), that is, at higher dilutions the second-order NLO response starts to be mainly controlled by the cationic part of the NLO chromophores, since the role of the counter anion no longer seems to be so relevant.

This behaviour is confirmed by the series of salts of **4** (Table 3 and Figure 2B). At 10^{-4} M, the $\mu\beta_{1.91}$ value reaches a common mean value around 1900×10^{-48} esu, independent of the nature of the counter anion. However, sulfonated anions, as expected for stronger ion pairing or for facile further aggregation of ion pairs, show a lower limiting $\mu\beta_{1.91}$ value of only 1150×10^{-48} esu. Major exceptions are provided by the salt with $[Hg_2I_6]^{2-}$, with a limiting $\mu\beta_{1.91}$ value of 6050×10^{-48} esu at 10^{-4} M, about three times that of the other salts (the high value is justified by the stoichiometry of the salt, which contains two NLO chromophores), and by the thiocyanate anion, with a high and constant $\mu\beta_{1.91}$ value of about 1850×10^{-48} esu that is not much dependent on concentration. We thus carried out some measurements on the iodide of **4**, at a concentration of about 10^{-2} M. As expected for increased H-type aggregation, as suggested by absorption spectroscopy, the $\mu\beta_{1.91}$ value decreases, reaching 1040×10^{-48} esu at 5×10^{-3} M and 925×10^{-48} esu at 10^{-2} M. (Tables 2 and 3).

We emphasise that the increase in $\mu\beta_{1.91}$ evidenced on dilution is not a result of inappropriate EFISH measurements, since the $\mu\beta_{1.91}$ value of *N*-(4-nitrophenyl)-L-prolinol (NPP), taken as reference remains unchanged even at 10^{-4} M concentration (see Figure 2B).

Starting from the evidence, obtained from dipole moment measurements, that at about 10^{-3} M the cationic NLO chromophores investigated herein are mainly associated as ion pairs, we calculated at this concentration the corresponding $\beta_{1.91}$ values and then the β_0 values for the iodides of **1**–**4** (Table 2) and for the various salts of **4** (Table 3). We can thus compare the EFISH β_0 value of the iodide of **3** with the β_0 values measured by the Stark-derived method on cationic NLO chromophore **3** in acetonitrile by Coe et al.[2] The EFISH β_0 value of 46.3×10^{-30} esu is, as expected for an ion pair, lower than the β_0 value of 90×10^{-30} esu reported by Coe et al. for the cationic chromophore using the Stark-derived method (the HRS value of 25×10^{-30} esu is probably underestimated).[2] Due to the different strength and size of the ion pairs formed by NLO chromophore **4** with various counter anions, the EFISH β_0 values of the various salts of **4** are quite dependent on the nature of the counter anion. These values are around $(17–22)\times10^{-30}$ esu for the salts with rather small counter anions such as $CF_3SO_3^-$ and ClO_4^-, and higher (around $(35–38)\times10^{-30}$ esu) for salts with larger counter anions such as $4\text{-}CH_3C_6H_4SO_3^-$ and *cis*-$[Ir(CO)_2I_2]^-$ (Table 3). Interestingly, for the salt of **4** with the thiocyanate counter anion, the EFISH β_0 value at 10^{-3} M is unexpectedly high (90.6×10^{-30} esu, Table 3). This high value would suggest a relatively high positive charge on the nitrogen atom of the pyridine ring, as confirmed by the large dipole moment (13 D) of the ion pair and by conductimetric measurements (see below).

In summary, the EFISH investigation has shown that in $CHCl_3$ solution the second-order NLO response of the salts of the cationic NLO chromophores **1**–**5** is controlled at about 10^{-3} M concentration by ion pairing, but on dilution to about 10^{-4} M or less it increases, as expected for progressive ionic dissociation of the ion pairs.[23] The slight decrease of the NLO response upon increasing the concentration above 10^{-3} M supports further aggregation of ion pairs to form H aggregates, as suggested by the effect of concentration on the electronic absorption spectra in solvents of low permittivity and confirmed by conductimetric and PGSE NMR investigations (see below). It follows that in a solvent of low dielectric constant like $CHCl_3$, the second-order NLO response of ionic NLO chromophores such as those investigated herein is strongly dependent upon concentration and upon the nature of the counter anion.

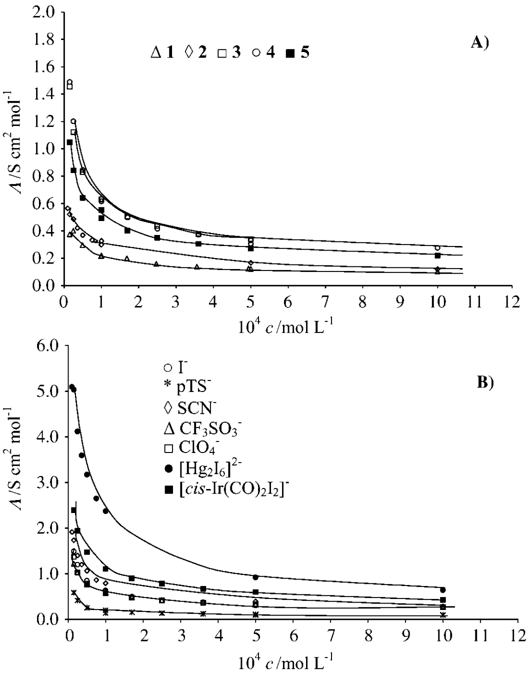

Figure 3. Plot of Λ versus molar concentration c for the iodides of **1**–**5** (A) and for the series of salts of **4** with various anions (B).

2.4. Conductimetric Investigation

To confirm that the increase in the second-order NLO response on dilution is due to increased ionic dissociation of the ion pairs, we carried out a careful conductimetric investigation in anhydrous $CHCl_3$ solution for at least six concentrations ranging from 10^{-5} M to 10^{-3} M. Tables 2 and 3 report the molar conductivities Λ.

Plots of the Λ values [obtained through Eqs. (8) and (9); see the Experimental Section] versus concentration for the iodides of **1**–**5** (Figure 3 A) and the series of salts of **4** with various counter anions (Figure 3 B) give information about the degree of dissociation. At concentrations between 10^{-4} M and 10^{-3} M, the Λ versus concentration plots for all salts are rather flat and with low values of Λ, which increase significantly with increasing dilution below 10^{-4} M. This trend, typical of extremely weak electrolytes, is evidence for an increased degree of ionic dissociation of ion pairs with increasing dilution.

The iodides of **1** and **2** are less conductive than the iodides of **3**, **4** and **5** over the entire range of concentrations (Figure 3 A), since for the former the lack of a strongly electron-donating substituent probably results in a higher positive charge on the nitrogen atom of pyridine ring, so that ion pairing is easier. The slightly lower Λ values over the entire range of concentrations of the iodide of **5** compared with those of **3** and **4** may indicate that lengthening of the π-delocalized bridge produces a decrease in mobility of the cation, due to its increased size.

Among the various salts of **4**, that with the $[Hg_2I_6]^{2-}$ anion shows the highest molar conductivity Λ and that with the anion $4\text{-}CH_3C_6H_4SO_3^-$ (pTS^-) the lowest over the entire range of concentrations (see Figure 3 B). For the former the high value of Λ is obviously due to its stoichiometry, while for the latter the low value of Λ suggests more facile ion pairing or further aggregation, in accordance with the EFISH investigation. The other salts of **4** show a trend of Λ versus concentration comparable to those of the iodides of **3** and **5**. The thiocyanate of **4** also starts to dissociate into ions, but only at concentrations well below 10^{-4} M (Figure 3 B).

The conductimetric data were analysed by applying the Kraus and Bray function [Eq. (1)],[24] useful to describe the behaviour of a weak electrolyte in solution:

$$\frac{1}{\Lambda}=\frac{1}{\Lambda^0}+\frac{c\Lambda}{K_a(\Lambda^0)^2} \qquad (1)$$

where K_a is the dissociation constant, and Λ^0 the molar conductivity at infinite dilution. For a weak uni-univalent electrolyte, the plot of $1/\Lambda$ versus $c\Lambda$ is a straight line, with intercept $1/\Lambda^0$. The degree of dissociation α of the weak electrolyte is given by Equation (2):

$$\alpha=\frac{\Lambda}{\Lambda^0} \qquad (2)$$

For all the salts investigated, the plot of the Kraus and Bray function (see Figure 4) in the range of the lower concentrations (between 10^{-5} M and 10^{-4} M) is a straight line, with very good linear correlation coefficients (between 0.965 and 0.999). Only at higher concentrations (more than 10^{-3} M) did we observe a deviation from linearity, suggesting the presence of aggregates of higher nuclearity.

In the range of concentrations typical for EFISH measurements (10^{-3}–10^{-4} M), the conductimetric data were also analysed by applying the Kraus and Fuoss function,[25] by plotting $\lg\Lambda$ versus $\lg c$. For ion pairs which dissociate into ions, the plot of $\lg\Lambda$ versus $\lg c$ should be a straight line with slope -0.5, while when the ion pairs associate into larger aggregates

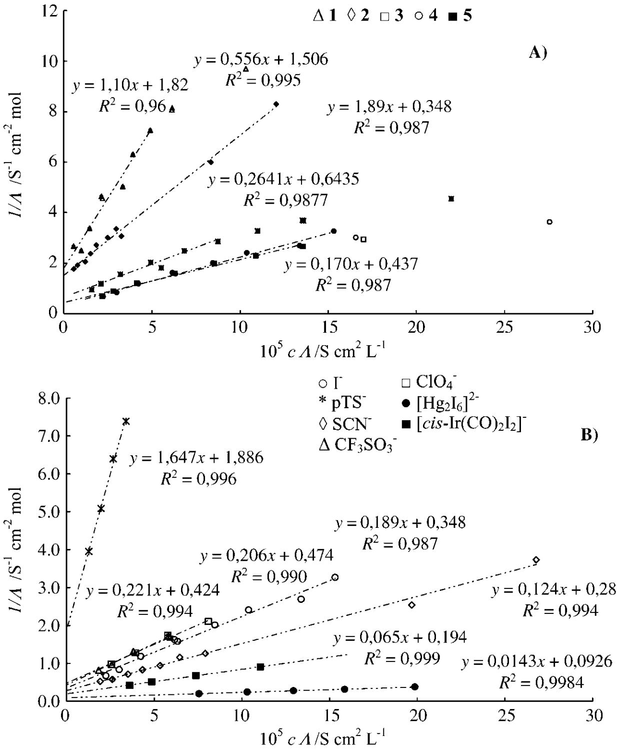

Figure 4. Plot of the Kraus and Bray function of the iodides of **1**–**5** (A) and various salts of **4** (B).

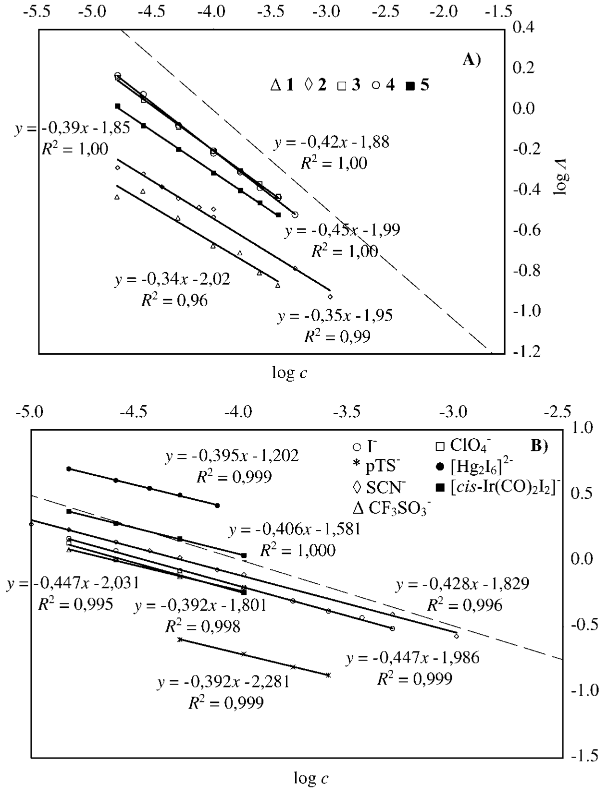

Figure 5. Plot of the Kraus and Fuoss function for the iodides of **1**–**5** (A) and various salts of **4** (B).

the slope of the plot decreases in absolute value and becomes positive. The Kraus and Fuoss plots for the iodides of **1**–**5** and for the various salts of **4** are reported in Figures 5 A and B, respectively.

All plots show deviations of the slopes from the decisive value of −0.5 at higher concentrations that confirm the presence of higher aggregates with increasing concentration. For the series of iodides (see Figure 5 A), a larger deviation is observed for **1** and **2** (the slope is about −0.34). This could be due to the lack of a substituent in the *para* position of the aromatic ring, which results in less steric hindrance and facilitates further aggregation.

For the various salts of **4**, on the other hand, a more significant deviation from a value of −0.5 is observed for the salt with the *p*-toluenesulfonate anion (pTS^-, slope = −0.39), while the slope for the salt with the thiocyanate anion is always quite near to the decisive value, thus confirming, in accordance with EFISH measurements, for the latter a strong and stable ion pair and for the former a significant tendency to aggregate to higher nuclearity species.

Figure 6 plots the ratio $\mu\beta_{1.91}/c$ versus α for all salts at concentrations below 10^{-3} M, in order to evidence a correlation between the second-order NLO response and the degree of dissociation. The plots for the iodides of **1**–**5** (Figure 6 A) and the various salts of **4** (Figure 6 B) show a good linear correlations $\mu\beta_{1.91}/c$ versus α for each salt, confirming a direct relation between the second-order NLO response and the degree of ionic dissociation.

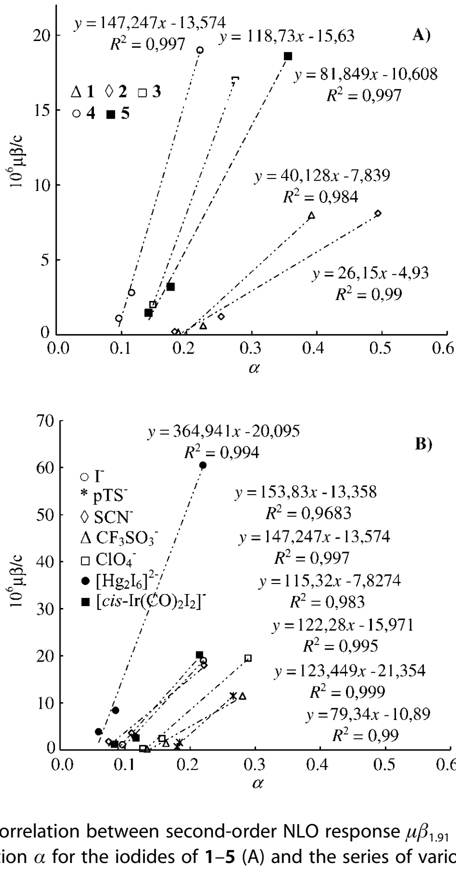

Figure 6. Correlation between second-order NLO response $\mu\beta_{1.91}$ and degree of dissociation α for the iodides of **1**–**5** (A) and the series of various salts of **4** (B).

2.5. PGSE NMR studies

Pulsed field gradient spin echo NMR measurements were carried out for the iodide and the *p*-toluenesulfonate of **4** in $CDCl_3$, as a function of concentration, in order to investigate the dissociation and aggregation processes in depth. Molecular hydrodynamic dimensions were derived from the experimentally measured translational self-diffusion coefficient D_t by using a modification of the Stokes–Einstein equation (3), which takes into account the pronounced elliptical shape of the pyridinium cation and of the ion pairs (Table 4):

$$D_t = \frac{kT}{fc\pi\eta\sqrt[3]{abd}} \tag{3}$$

In Equation (3), $\sqrt[3]{abd}$ replaces the hydrodynamic radius r_H, k is the Boltzman constant, T the absolute temperature, η the fluid viscosity, c the "size factor", f the "shape factor", and a, b and d are the semi-axes of the ellipsoid ($a > b > d$).[12] From the D_t values the structural parameter P, defined as $kT/\pi\eta D_t = f_s c\sqrt[3]{abd}$, was obtained (Table 4). Since both f and c can be expressed as a function of a, b, and d,[26] the structural parameter P for the cation (P^+) was computed by using a, b and d parameters of the ellipsoid that better fit the modelled van der Waals surface of cation **4** ($2a = 21.2$, $2b = 9.2$, $2d = 5.4$ Å, Figure 7 A) and the hydrodynamic radius of the solvent (2.60 and 2.67 Å for $CDCl_3$ and DMSO, respectively). The choice of these structural parameters was confirmed by the calculated value of P (29.63 Å), in excellent agreement with the experimental value obtained in DMSO (29.46 Å, average value of entries 12 and 13 in Table 4). In this solvent it is known that salts are prevalently dissociated into free ions. By positioning the iodide anion in front of positively charged nitrogen atom of the pyridinium ring in the ion pair structure, a P value for the ion pair (P^{IP}) of 33.46 in $CDCl_3$ was calculated ($2a = 25.4$, $2b = 9.2$ and $2d = 5.4$ Å; ionic radius of $I^- = 2.11$ Å[27]).

Comparison of the experimental P values in CD_3Cl reported in Table 4 with the calculated P^{IP} for the iodide of **4** indicates that only at the two lower concentrations (7.7×10^{-5} and 2.64×10^{-4} M) are the values of P smaller than P^{IP}, that is, at these concentrations ion pairs start to be sufficiently dissociated into free ions. In agreement with the previous conductivity investigation, at concentrations on the order of 10^{-3} M or higher, the experimental P value becomes greater than P^{IP}, and this confirms that ion pairs start to associate to form higher aggregates. This self-aggregation of the iodide of **4** can be thus evaluated by introducing the aggregation number N, defined as the average number of ion pairs per aggregate. To evaluate N some hypotheses must be made concerning the structures of the aggregates. Two limit models can be taken into account: ion pairs stack as H aggregates (AG1) or form a head to tail polymer (AG2; Figure 7 B). In the AG1 model, $2a$ and $2b$ parameters of the ellipsoid remain constant while $2d$ increases (up to L1) as a consequence of aggregation. Instead, only $2a$ changes (up to L2) in the aggregation process for model AG2. Thus, P values were calculated for the AG1 and AG2 models while varying only the $2d$ and $2a$ parameters, respectively, so that N values could be obtained as the ratios of L1/$2d$ and L2/$2a$ for AG1 (N^{+AG1}) and AG2 (N^{+AG2}), respectively (Table 4). N^{+AG1} and N^{+AG2} span from 1 to 3.8 and from 1 to 1.9, respectively. It is not surprising that $N^{+AG1} > N^{+AG2}$, since the former has a more spherical shape.

Table 4. Diffusion coefficient ($10^{-10} D_t$ [$m^2 s^{-1}$]), structural parameter P [Å], and aggregation numbers N for the iodide and the *p*-toluenesulfonate of **4** in $CDCl_3$ and DMSO as a function of concentration C [M].

Entry	Solvent	C	D_t^+	D_t^-	P^+	P^-	N^{+AG1}	N^{-AG1}	N^{+AG2}	N^{-AG2}
					iodide					
1	$CDCl_3$	7.7×10^{-5}	7.07		32.65		0.9	0.7	0.9	0.7
2	$CDCl_3$	2.64×10^{-4}	6.94		33.19		0.9	0.9	0.9	0.9
3	$CDCl_3$	7.93×10^{-4}	6.83		33.73		1.0		1.0	
4	$CDCl_3$	1.76×10^{-3}	6.59		35.00		1.1		1.0	
5	$CDCl_3$	4.4×10^{-3}	6.10		37.83		1.5		1.2	
6	$CDCl_3$	6.71×10^{-3}	5.93		38.89		1.7		1.2	
7	$CDCl_3$	9.12×10^{-3}	5.80		39.76		1.8		1.3	
8	$CDCl_3$	1.53×10^{-2}	5.44		42.44		2.2		1.4	
9	$CDCl_3$	2.79×10^{-2}	5.17		44.61		2.5		1.5	
10	$CDCl_3$	4.73×10^{-2}	4.81		47.97		3.1		1.7	
11	$CDCl_3$	9.31×10^{-2}	4.43		52.04		3.8		1.9	
12	DMSO	1.76×10^{-4}	2.08		29.35					
13	DMSO	5.55×10^{-3}	2.06		29.58					
					p-toluenesulfonate					
14	$CDCl_3$	6×10^{-6}	6.76	7.10	32.83	31.23	0.8	0.5	0.8	0.5
15	$CDCl_3$	3.9×10^{-5}	6.40	6.68	34.57	33.15	0.8	0.7	0.8	0.7
16	$CDCl_3$	3.09×10^{-4}	6.27	6.34	35.49	35.08	0.9	0.8	0.9	0.8
17	$CDCl_3$	1.02×10^{-3}	5.92	5.94	37.37	37.21	1.0	1.0	1.0	1.0
18	$CDCl_3$	1.86×10^{-3}	5.83	5.82	38.10	38.17	1.1	1.1	1.0	1.0
19	$CDCl_3$	3.62×10^{-3}	5.78	5.78	39.66	39.68	1.3	1.3	1.1	1.1
20	$CDCl_3$	6.94×10^{-3}	5.60	5.52	41.46	42.09	1.5	1.5	1.1	1.2
21	$CDCl_3$	1.54×10^{-2}	5.09	5.05	45.31	45.72	2.0	2.1	1.3	1.3
22	DMSO	2.91×10^{-3}	2.06	3.59	29.629	16.967				

In the case of the *p*-toluenesulfonate of **4**, it can be reasonably assumed that in the ion-pair structure the polar SO_3^- head of the anion approaches the positively charged pyridine nitrogen atom of the cation, as suggested for similar ion pairs by Grunwald and co-workers.[15,16] Two limit situations can thus occur: the methyl group of the *p*-toluenesulfonate anion is oriented toward the NBu_2 substituent (structure A) or in the opposite direction (structure B).[28–31] To discriminate between these two structures, the inter-ionic structure of the ion pair of the *p*-toluenesulfonate of **4** was investigated by recording a series of ^1H NOESY NMR spectra[32] at different concentrations (1.02×10^{-3}, 6.94×10^{-3} and 1.54×10^{-2} M) in $CDCl_3$. Very weak interionic contacts could be detected only for the more

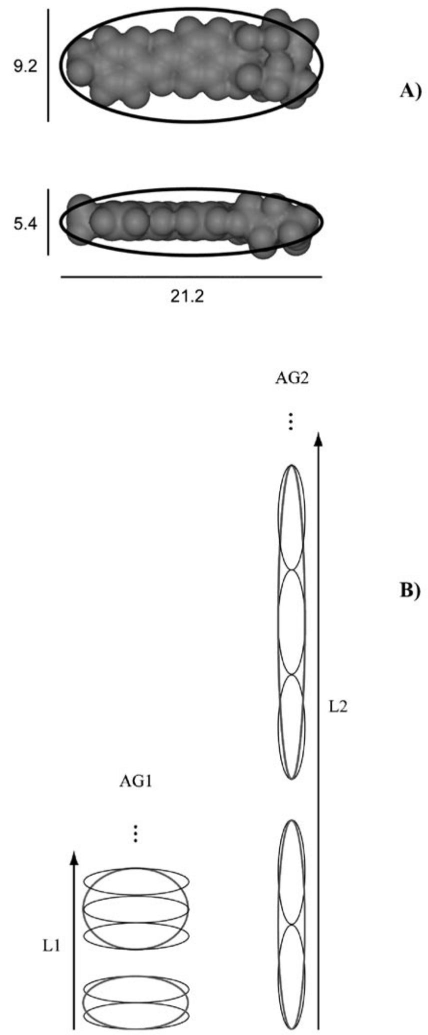

Figure 7. Lateral and top views of the van der Waals surfaces of cationic NLO chromophore **4** with structural parameters [Å] of the ellipsoid used as geometrical model for PGSE NMR data analysis (A) and two models for the aggregation of monomers (black) into dimers, trimers and higher aggregates (red) (B).

concentrated solution. In particular, the hydrogen atoms in *ortho* position to the SO_3^- group of the anion interact with the methyl protons of the methylpyridinium group and with those in the 2,6-positions of the pyridine ring (see Figure 1 for the numbering scheme). Interionic contacts were not observed for any other resonance of the cation, and thus structure B is confirmed. A value of 37.24 Å ($2a=30$, $2b=9.2$, $2d=5.4$ Å) was thus calculated for P^{IP} of the ion pair with structure B. The N^{+AG1} and N^{+AG2} values for the two models of aggregation of ion pairs, reported in Figure 8, were calculated as described above. Since in the case of the *p*-toluenesulfonate of **4**, also the counter anion has some protons, it was possible to evaluate D_t, P and N values for both the cation and the anion (Table 4). Interestingly, for concentrations higher than 3.09×10^{-4} M, cation and anion translate, as expected for an ion pair, as a whole object, since D_t^+ and D_t^-, P^+ and P^- and N^+ and N^- show similar values.

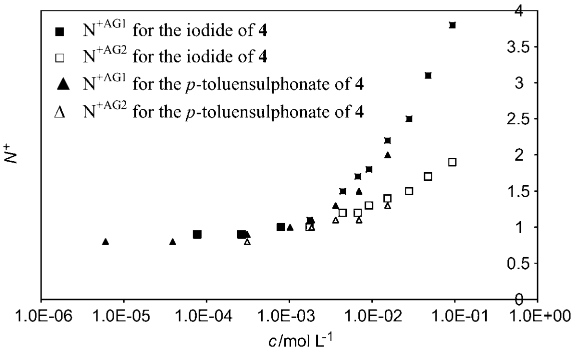

Figure 8. Aggregation numbers for the iodide and the *p*-toluenesulfonate of **4** as a function of concentration in $CDCl_3$.

The *N* values as a function of concentration for the iodide and the *p*-toluenesulfonate of **4** follow substantially the same trends (Figure 8), although the *p*-toluenesulfonate shows a slightly larger tendency to aggregate. At least in model AG1, it seems that self-aggregation proceeds beyond ion quadruples;[33] the AG1 model corresponds to the more probable H-type aggregation, as suggested by EFISH measurements and solvent effects on the electronic absorption spectra. Assuming that ion pairs undergo indefinite self-aggregation following the isodesmic model,[34] an estimate of the equilibrium aggregation constant K_{AGG} can be obtained by the relationship: $N(N-1)=K_{AGG}C$.[35] Taking into account concentrations higher than 5×10^{-4} M, where the concentration of free ions becomes small, the following K_{AGG} values are obtained: iodide of **4** (AG2): 19 ± 2, iodide of **4** (AG1): 118 ± 6, *p*-toluenesulfonate of **4** (AG2): 32 ± 1, *p*-toluenesulfonate of **4** (AG1): 154 ± 6 M^{-1}.

The greater tendency of the *p*-toluenesulfonate of **4** to form aggregates compared to the iodide of **4** is in agreement with the evidence provided by the Krauss and Fuoss plots of Figure 5.

3. Conclusions

We have reported evidences based on dipole-moment measurements and conductimetric and PGSE NMR investigations that 4-X-1-methylpyridinium salts in anhydrous $CHCl_3$ solution are associated as ion pairs in the range of concentration around 5×10^{-4}–10^{-3} M. At lower concentrations, significant dissociation into ions takes place, while at higher concentration ion pairs become associated into larger aggregates, probably of H type. For the second-order cationic NLO chromophore **4**, dissociation into free ions and association to form higher aggregates has been shown to be controlled by the nature of the counter anion.

It follows that the second-order NLO response of the pyridinium salts investigated here strongly depends upon the nature of the counter anion and also upon concentration. Below 5×10^{-4} M, the ion pairs start to dissociate into ions with a strong increase in second-order NLO response $\mu\beta_{1.91}$, measured by the EFISH technique. An unexpected exception (a rather constant $\mu\beta_{1.91}$ value) was found when thiocyanate is the counter anion of **4**, but conductivity measurements in anhydrous $CHCl_3$ confirmed that the thiocyanate of **4** shows in the range of concentration investigated (10^{-4}–10^{-3} M) trends typical of a tight ion pair which does not easily dissociate. Salts of **4** with sulfonated anions such as $CF_3SO_3^-$ and *p*-toluenesulfonate show a significant tendency to form stronger ion pairs and higher aggregates, while salts with other counter anions such as I^-, ClO_4^-, $[Hg_2I_6]^{2-}$ and *cis*-$[Ir(CO)_2I_2]^-$ show a minor tendency to ion pairing. This group, with increasing dilution, shows increased dissociation into free ions, with higher second-order NLO response $\mu\beta_{1.91}$, which finally becomes quite independent of the nature of the counter anion.

In conclusion, our multidisciplinary investigation has shown that, when working in a solvent of low electrical permittivity such as anhydrous $CHCl_3$, the second-order NLO response of 4-X-1-methylpyridinium second-order cationic NLO chromophores depends on concentration and on the nature of the counter anion. Therefore, such dependence cannot be neglected and should be carefully taken into consideration.

Experimental Section

General Comments: $IrCl_3$ was purchased from Engelhardt. Iodomethane, methyl trifluoromethanesulfonate, all silver salts ($AgClO_4$, $AgCF_3SO_3$, $Ag(4\text{-}CH_3C_6H_4SO_3)$, AgSCN), mercury (II) iodide, stilbazolic ligands **a** and **c** (Figure 1), the iodides of **3** and **4** (Table 1) and all solvents were purchased from Sigma-Aldrich and used without further purification, whereas stilbazoles **b**[17a] and **d**[17b] (Figure 1) and $[Ir(COT)_2Cl]_2$[13] (COT = cyclooctene) were synthesized according to the literature. All the other salts investigated, with the exception of the iodides of **3** and **4** (Table 1), were prepared as described below, under a nitrogen atmosphere, by using flasks previously dried over flame and cooled under nitrogen flow. Carefully dried $CHCl_3$ stabilized with amylene was used for measurements of dipole moment, electronic absorption and emission spectra, EFISH and conductivity. All products were characterized by ^1H NMR (Bruker DRX-300 spectrometer; see Figure 1 for atom numbering) and elemental analysis. Electronic absorption spectra were recorded on a Jasco V-530 spectrophotometer, and emission spectra on a JASCO FP-777 spectrofluorimeter. Dipole moments μ were measured by using a WTW-DM01 dipole meter (dielectric constant) coupled with an RX-5000 ATAGO Digital Refractometer (refractive index) according to the Guggenheim method.[14] Elemental analyses were carried out at the Dipartimento di Chimica Inorganica, Metallorganica e Analitica "Lamberto Malatesta" of the Università di Milano.

EFISH Measurements: The molecular quadratic hyperpolarizabilities of the 4-X-1-methylpyridinium salts investigated in this work (Table 1) were obtained by the solution-phase dc electric field induced second harmonic (EFISH) generation technique,[6] which can provide direct information on the intrinsic molecular second-order NLO properties through Equation (4):

$$\gamma_{\text{EFISH}} = (\mu\beta_\lambda / 5\,kT) + \gamma(-2\,\omega;\,\omega,\,\omega,\,0) \tag{4}$$

where $\mu\beta_\lambda/5\,kT$ represents the dipolar orientational contribution and $\gamma(-2\omega;\,\omega,\,\omega,\,0)$, a third-order term at frequency ω of the incident wavelength, is the electronic contribution to γ_{EFISH}, which is negligible for the kind of molecules investigated herein.[17b,19] β_λ is the projection along the dipole moment axis of the vectorial component β_{VEC} of the tensor of the quadratic hyperpolarizability at incident wavelength λ. All EFISH measurements were carried out at the Dipartimento di Chimica Inorganica Metallorganica e Analitica "Lamberto Malatesta" of the Università di Milano, on$CHCl_3$ solutions of different concentrations (usually 10^{-3}, 5×10^{-4} and 10^{-4} M) at a non-resonant incident wavelength of 1.907 µm (simplified as 1.91 µm), obtained by Raman-shifting the fundamental 1.064 µm wavelength produced by a Q-switched, mode-locked Nd^{3+}:YAG laser.

Dipole-Moment Measurements: Dipole moments were evaluated in $CHCl_3$ solutions by means of the Guggenheim method.[14] Referring to the solvent as 1 and to the solute as 2, the value of μ (expressed in Debye) is obtained from the orientational polarization of the solute $_\mu P_2$ through Equation (5):

$$\mu = \sqrt{\frac{9kT}{4\pi N_a}}\sqrt{_\mu P_2 T} = 0.012813\sqrt{_\mu P_2 T} \tag{5}$$

The orientational polarization is determined by Equation (6):

$$_\mu P_2 = \frac{3M_2}{d_1(\varepsilon_1 + 2)^2}(\alpha - \nu) \tag{6}$$

where M_2 is the molecular weight of the solute, d_1 the density of the solvent, ε_1 its dielectric constant and α and ν are, respectively, the slopes of the straight-line plots of dielectric constant versus concentration and the square root of the refractive index versus concentration of solutions at various concentration of the solute.

The dielectric constant is linearly related to the physically measurable capacity C of the solution by Equation (7):

$$\varepsilon = a + bC \tag{7}$$

The coefficients a and b were obtained by calibration of the dipole meter with a series of pure solvents (in our case $CHCl_3$, chlorobenzene and ethyl acetate) of known dielectric constant ε.

For each salt five solutions in $CHCl_3$ were prepared and measured working in a concentration range of 10^{-4}–10^{-3} M, characterized by strong ion pairing. In all cases extremely good linear plots were obtained, confirming that ionic dissociation of strong ion pairs is not relevant in the range of concentrations investigated. For example, Figure 9 shows the linear plots of dielectric constant versus concentration and square of the refractive index versus concentration for the salt of **4** with the triflate anion.

Electrical conductivity measurements were carried out in $CHCl_3$ solutions at concentrations ranging from 10^{-5} to 10^{-3} M, the upper value being determined by the solubility of the salts, and the lower by the instrumental limits. All measurements were carried out at 298 K with an AMEL 160 conductimeter, equipped with an immersion cell with platinated platinum electrodes and glass insulating parts, characterized by a cell constant of ca. 1 (exactly established at the beginning of the experimental work by using an aqueous 0.01 M KCl solution as standard). The conductance G of the pure solvent ($5\times10^{-9}\ \Omega^{-1}$) was determined before each set of experiments and subsequently subtracted from the conductance measured for the solutions.

Molar conductivity Λ is given by Equation 8:

$$\Lambda = \frac{1000\kappa}{c} \tag{8}$$

where c is the concentration of the solution (in mol dm^{-3}) and κ the specific conductivity (in $\Omega^{-1}\,cm^{-1}$), directly obtained by the experimental measure of the conductance G through Equation (9):

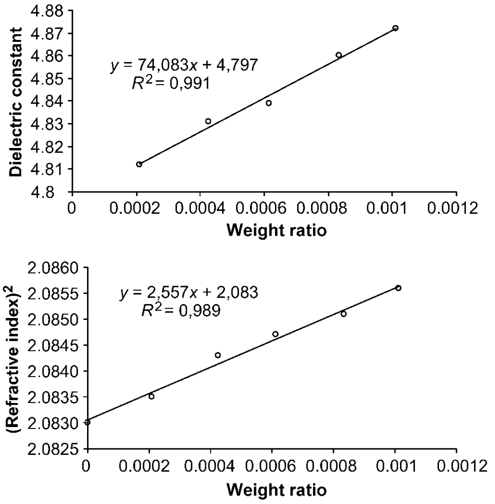

Figure 9. An example of the good linear correlation of the dielectric constant and square of the refractive index versus concentration (weight ratio of solute to solvent) for the salt of **4** with triflate counter anion.

$$G = \frac{1}{\kappa}\frac{L}{S} \qquad (9)$$

where *L/S* is the cell constant.

PGSE Diffusion NMR Measurements: PGSE NMR measurements were performed on a Bruker Avance DRX 400 spectrometer equipped with a direct QNP probe and a *z*-gradient coil controlled by a Great 1/10 gradient unit, by using the standard stimulated echo pulse sequence[36] at 295 K without spinning. The dependence of the resonance intensity *I* on a constant waiting time and on a varied gradient strength *G* is described by Equation (10):

$$\ln\frac{I}{I_0} = -(\delta\gamma)^2 D_t\left(\varDelta - \frac{\delta}{3}\right)G^2 \qquad (10)$$

where *I* is the intensity of the observed spin echo, I_0 the intensity of the spin echo without gradients, D_t the translational self-diffusion coefficient, $\varDelta$ the delay between the midpoints of the gradients, δ the length of the gradient pulse and γ the magnetogyric ratio. The shape of the gradients was rectangular, their duration δ was 4 ms and their strength *G* was varied during the experiments. ^{1}H PGSE NMR spectra were acquired with 32 K points, 16, 32, 64, 128, 256, 512 or 3072 scans, depending on concentration, and a spectral width of 5000 Hz. All spectra were processed with a line broadening of 1.0 Hz. The semi-logarithmic plots of ln(I/I_0) versus G^2 were fitted by using a standard linear regression algorithm to give an *R* factor always better than 0.99. Gradients were calibrated on the diffusion of HDO in D_2O;[37] data at different temperatures were estimated by interpolation of the data reported by Mills, giving $D_{HDO} = 1.748 \times 10^{-9}$ m^2 s^{-1} at 295 K. The residual resonance of $CHCl_3$ was used as internal standard. The uncertainty in measurements of D_t was estimated by determining the standard deviation of D_t by performing experiments with different diffusion times $\varDelta$. The standard propagation of error analysis gave a standard deviation of approximately 3–4% for D_t and a consequent error of 9–12% for the value of the aggregation number *N*. Only four gradients were used for the measurements carried out for the *p*-toluenesulfonate of **4** at the lowest concentration (ca. 6×10^{-6} M); consequently, the error in the corresponding D_t is slightly higher (around 5–8%).

(*E*)-4-Styryl-1-methylpyridinium Iodide: A solution of iodomethane (2.49 mL; 40 mmol) in toluene (2 mL) was added dropwise to a solution of stilbazole **a** (200 mg; 1.1 mmol) in toluene (6 mL). Vigorous stirring for 2 h at room temperature in the dark (aluminium foil) afforded a yellow solid, which was dissolved in CH_3CN and precipitated by addition of Et_2O at room temperature to give 230 mg of the iodide of **1** (65%) as a yellow powder. ^{1}H NMR (300 MHz, $CDCl_3$, 25 °C, TMS): δ = 9.02 (d, ^3J(H,H) = 6.6 Hz, 2H; H^2, H^6), 8.04 (d, ^3J(H,H) = 6.5 Hz, 2H; H^3, H^5), 7.72 (d, ^3J(H,H) = 16.3 Hz, 1H; H^7), 7.66 (m, 2H; H^{10}, H^{14}), 7.48 (m, 3H; H^{11}, H^{12}, H^{13}), 7.18 (d, ^3J(H,H) = 16.1 Hz, 1H; H$_8$), 4.58 (s, 3H; NCH_3): elemental analysis (%) calcd (found): C 52.03 (52.05), H 4.37 (4.33), N 4.33 (4.40).

(*E*)-4-(4′-*tert*-Butylstyryl)-1-methylpyridinium Iodide: A solution of iodomethane (0.66 mL; 10.6 mmol) in CH_2Cl_2 (2 mL) was added dropwise to a solution of stilbazole **b** (50 mg; 0.21 mmol) in CH_2Cl_2 (18 mL). Vigorous stirring for 2 h at room temperature in the dark (aluminium foil) afforded a yellow solid, which was dissolved in CH_2Cl_2 and precipitated by addition of *n*-hexane at room temperature to give 59.7 mg of the iodide of **2** (75%) as a yellow powder. ^{1}H NMR (300 MHz, $CDCl_3$, 25 °C, TMS): δ = 8.98 (d, ^3J(H,H) = 6.7 Hz, 2H; H^2, H^6), 7.99 (d, ^3J(H,H) = 6.8 Hz, 2H; H^3, H^5), 7.70 (d, ^3J(H,H) = 16.2 Hz, 1H; H^7), 7.60 (d, ^3J(H,H) = 8.4 Hz, 2H; H^{10}, H^{14}), 7.50 (d, ^3J(H,H) = 8.5 Hz, 2H; H^{11}, H^{13}), 7.13 (d, ^3J(H,H) = 16.2 Hz, 1H; H$_8$), 4.57 (s, 3H; NCH_3), 2.19 (s, 9H; $C(CH_3)_3$): elemental analysis (%) calcd (found): C 57.00 (57.03), H 5.85 (5.78), N 3.69 (3.72).

(*E,E*)-4-[4′-(Dimethylaminophenyl)-1,3-butadienyl]-1-methylpyridinium Iodide: A solution of iodomethane (1.86 mL; 29.9 mmol) in CH_2Cl_2 (2 mL) was added dropwise to a solution of stilbazole **d** (150 mg; 0.6 mmol) in CH_2Cl_2 (68 mL). Vigorous stirring for 2 h at room temperature in the dark (aluminium foil) afforded a red solid, which was dissolved in CH_2Cl_2 and precipitated by addition of *n*-hexane at room temperature to give 145 mg of the iodide of **5** (62%) as a pale violet powder. ^{1}H NMR (300 MHz, $CDCl_3$, 25 °C, TMS): δ = 8.97 (d, ^3J(H,H) = 6.5 Hz, 2H; H^2, H^6), 7.77 (d, ^3J(H,H) = 6.5 Hz, 2H; H^3, H^5), 7.52 (dd, ^3J(H,H) = 10.7 Hz, ^3J(H,H) = 15.1 Hz, 1H; H$_8$), 7.46 (d, ^3J(H,H) = 8.9 Hz, 2H; H^{12}, H^{16}), 7.04 (d, ^3J(H,H) = 15.2 Hz, 1H; H^{10}), 6.90 (dd, ^3J(H,H) = 10.7 Hz, ^3J(H,H) = 15.2 Hz, 1H; H$_9$), 6.81 (m, 2H; H^{13}, H^{15}), 6.55 (d, ^3J(H,H) = 15.2 Hz, 1H; H^7), 4.54 (s, 3H; NCH_3), 3.08 (s, 6H; $N(CH_3)_2$): elemental analysis (%) calcd (found): C 55.11 (55.36), H 5.39 (5.25), N 7.14 (7.44).

(*E*)-4-[4′-(Dibutylamino)styryl)]-1-methylpyridinium Trifluoromethanesulfonate: A solution of $Ag(CF_3SO_3)$ (114 mg, 0.444 mmol) in CH_3CN (10 mL) was added dropwise at room temperature to a solution of the iodide of **4** (200 mg, 0.444 mmol) in CH_3CN (40 mL). The reaction mixture was stirred at room temperature in the dark (aluminium foil) for 1 h, and then AgI was filtered off. Evaporation of the filtrate gave a red powder, which was dissolved in CH_2Cl_2 and precipitated by addition of *n*-hexane at room temperature to afford 185 mg of the triflate of **4** (88%) as a red powder. ^{1}H NMR (300 MHz, $CDCl_3$, 25 °C, TMS): δ = 8.44 (d, ^3J(H,H) = 6.8 Hz, 2H; H^2, H^6), 7.74 (d, ^3J(H,H) = 6.8 Hz, 2H; H^3, H^5), 7.57 (d, ^3J(H,H) = 15.8 Hz, 1H; H$_8$), 7.49 (d, ^3J(H,H) = 8.8 Hz, 2H; H^{10}, H^{14}), 6.79 (d, ^3J(H,H) = 15.8 Hz, 1H; H^7), 6.66 (d, ^3J(H,H) = 8.8 Hz, 2H; H^{11}, H^{13}), 4.25 (s, 3H; NCH_3), 3.36 (t, ^3J(H,H) = 7.3 Hz, 4H; NCH_2), 1.61 (m, 4H; CH_2), 1.32 (m, 4H; CH_2), 0.92 (t, ^3J(H,H) = 7.2 Hz, 6H; CH_3): elemental analysis (%) calcd (found): C 58.46 (58.52), H 6.61 (6.44), N 5.93 (6.04).

(*E*)-4-[4′(-Dibutylamino)styryl]-1-methylpyridinium Perchlorate: A solution of $AgClO_4$ (92 mg, 0.444 mmol) in CH_3CN (20 mL) was added dropwise at room temperature to a solution of the iodide of **4** (200 mg, 0.444 mmol) in CH_3CN (80 mL). The reaction mixture was stirred at room temperature in the dark (aluminium foil) for 1 h, and then AgI was filtered off. Evaporation of the filtrate gave an orange powder, which was dissolved in CH_2Cl_2 and precipitated by addition of *n*-hexane at room temperature to afford 150 mg of the perchlorate of **4** (80%) as an orange powder. ^{1}H NMR (300 MHz, $CDCl_3$, 25 °C, TMS): $\delta = 8.37$ (d, ^3J(H,H) = 6.8 Hz, 2H; H^2, H^6), 7.75 (d, ^3J(H,H) = 6.8 Hz, 2H; H^3, H^5), 7.58 (d, ^3J(H,H) = 15.9 Hz, 1H; H$_8$), 7.50 (d, ^3J(H,H) = 8.8 Hz, 2H; H^{10}, H^{14}), 6.80 (d, ^3J(H,H) = 15.9 Hz, 1H; H^7), 6.66 (d, ^3J(H,H) = 8.4 Hz, 2H; H^{11}, H^{13}), 4.27 (s, 3H; NCH_3), 3.36 (t, ^3J(H,H) = 7.8 Hz, 4H; NCH_2-), 1.61 (m, 4H; CH_2), 1.40 (m, 4H; CH_2), 0.99 (t, ^3J(H,H) = 7.2 Hz, 6H; CH_3): elemental analysis (%) calcd (found): C 62.47 (62.53), H 7.39 (7.41), N 6.42 (6.37).

(*E*)-4-[4′-(Dibutylamino)styryl]-1-methylpyridinium Thiocyanate: Solid AgSCN (74 mg, 0.444 mmol) was added at room temperature to a solution of the iodide of **4** (200 mg, 0.444 mmol) in CH_3CN (40 mL). The reaction mixture was stirred at room temperature in the dark (aluminium foil) for 5 d, and then AgI was filtered off. Evaporation of the filtrate gave a red powder, which was dissolved in CH_3CN and precipitated by addition of *n*-hexane at room temperature to afford 129 mg of the thiocyanate of **4** (76%), as a red powder. ^{1}H NMR (300 MHz, $CDCl_3$, 25 °C, TMS): $\delta = 8.52$ (d, ^3J(H,H) = 6.4 Hz, 2H; H^2, H^6), 7.81 (d, ^3J(H,H) = 6.5 Hz, 2H; H^3, H^5), 7.64 (d, ^3J(H,H) = 15.9 Hz, 1H; H$_8$), 7.51 (d, ^3J(H,H) = 8.9 Hz, 2H; H^{10}, H^{14}), 6.83 (d, ^3J(H,H) = 15.8 Hz, 1H; H^7), 6.66 (d, ^3J(H,H) = 9.0 Hz, 2H; H^{11}, H^{13}), 4.40 (s, 3H; NCH_3), 3.37 (t, ^3J(H,H) = 7.5 Hz, 4H; NCH_2), 1.63 (m, 4H; CH-), 1.40 (m, 4H; CH_2), 0.99 (t, ^3J(H,H) = 7.3 Hz, 6H; CH_3): elemental analysis (%) calcd (found): C 72.40 (72.35), H 8.19 (8.24), N 11.01 (11.05).

(*E*)-4-[4′-(Dibutylamino)styryl]-1-methylpyridinium *p*-Toluenesulfonate: A solution of Ag(4-$CH_3C_6H_4SO_3$) (152 mg, 0.546 mmol) in CH_3CN (10 mL) was added dropwise at room temperature to a solution of the iodide of **4** (246 mg, 0.546 mmol) in CH_3CN (40 mL). The reaction mixture was stirred at room temperature in the dark (aluminium foil) for 3 h, and then AgI was filtered off. Evaporation of the filtrate gave a red powder, which was dissolved in CH_3CN and precipitated by addition of *n*-hexane at room temperature to afford 150 mg of the *p*-toluenesulfonate of **4** (68%), as a red powder. ^{1}H NMR (300 MHz, $CDCl_3$, 25 °C, TMS): $\delta = 8.71$ (d, ^3J(H,H) = 6.5 Hz, 2H; H^2, H^6), 7.82 (d, ^3J(H,H) = 8.1 Hz, 2H; H *ortho* to CH_3 of the anion), 7.74 (m, 2H; H^3, H^5), 7.49 (m, 3H; H$_8$, H^{10}, H^{14}), 7.14 (d, ^3J(H,H) = 7.9 Hz, 2H; H *ortho* to SO_3 of the anion), 6.75 (brm, 3H; H^7, H^{11}, H^{13}), 4.44 (s, 3H; NCH_3), 3.40 (t, ^3J(H,H) = 6.9 Hz, 4H; NCH_2-), 2.35 (s, 3H; CH_3 of the anion), 1.61 (m, 4H; CH_2), 1.35 (m, 4H; CH_2), 0.92 (t, ^3J(H,H) = 7.2 Hz, 6H; CH_3): elemental analysis (%) calcd (found): C 70.41 (70.29), H 7.74 (7.70), N 5.66 (5.36).

(*E*)-4-[4′-(Dibutylamino)styryl]-1-methylpyridinium Hexaiododimercurate: A solution of HgI_2 (100 mg, 0.222 mmol) in EtOH (20 mL) was added dropwise at room temperature to a solution of the iodide of **4** (200 mg, 0.444 mmol) in EtOH (70 mL). The reaction mixture was stirred at room temperature in the dark (aluminium foil) for 1 h, affording a red precipitate, which was dissolved in CH_2Cl_2 and precipitated by addition of *n*-hexane at room temperature to give 189 mg of the hexaiododimercurate of **4** (47%), as a red powder. ^{1}H NMR (300 MHz, $CDCl_3$, 25 °C, TMS): $\delta = 8.39$ (d, ^3J(H,H) = 6.6 Hz, 2H; H^2, H^6), 7.82 (d, ^3J(H,H) = 6.6 Hz, 2H; H^3, H^5), 7.68 (d, ^3J(H,H) = 15.8 Hz, 1H; H$_8$), 7.54 (d, ^3J(H,H) = 8.8 Hz, 2H; H^{10}, H^{14}), 6.86 (d, ^3J(H,H) = 15.8 Hz, 1H; H^7), 6.68 (d, ^3J(H,H) = 8.2 Hz, 2H; H^{11}, H^{13}), 4.34 (s, 3H; CH_3), 3.38 (t, ^3J(H,H) = 7.6 Hz, 4H; NCH_2), 1.61 (m, 4H; CH_2), 1.40 (m, 4H; CH_2), 0.99 (t, ^3J(H,H) = 7.2 Hz, 6H; CH_3): elemental analysis (%) calcd (found): C 29.20 (29.12), H 3.45 (3.39), N 3.10 (3.15).

(*E*)-4-[4′-(Dibutylamino)styryl]-1-methylpyridinium *cis*-dicarbonyldiiodoiridate(I): A stream of CO was bubbled into a solution of [{Ir(COT)$_2$Cl}$_2$] (417 mg, 0.466 mmol) in degassed EtOH (80 mL), leading to precipitation of [Ir(CO)$_2$Cl]$_n$ as a black powder. KI (298.5 mg, 1.86 mmol) was added and the reaction mixture was heated to reflux for 90 min. The yellow-green solution was cooled to room temperature and KCl filtered off. After removal of the solvent in vacuo, K[Ir(CO)$_2$I$_2$] was recovered as a dark brown powder. A suspension of K[Ir(CO)$_2$I$_2$] (480 mg, 0.888 mmol) in degassed distilled H_2O (80 mL) was then added to a solution of the iodide of **4** (400 mg, 0.888 mmol) in CH_2Cl_2 (50 mL) and the mixture was left at room temperature with vigorous stirring for 24 hrs. The layers were separated and the organic layer washed with H_2O (3×25 mL), dried over Na_2SO_4 and evaporated, affording 300 mg of the *cis*-dicarbonyldiiodoiridate(I) of **4** (41% with respect to the iodide of **4**) as a dark orange powder. ^{1}H NMR (300 MHz, CD_2Cl_2, 25 °C, TMS): $\delta = 8.33$ (d, ^3J(H,H) = 6.8 Hz, 2H; H^2, H^6), 7.82 (d, ^3J(H,H) = 6.8 Hz, 2H; H^3, H^5), 7.70 (d, ^3J(H,H) = 15.8 Hz, 1H; H$_8$), 7.57 (d, ^3J(H,H) = 9.0 Hz, 2H; H^{10}, H^{14}), 6.91 (d, ^3J(H,H) = 15.8 Hz, 1H; H^7), 6.72 (d, ^3J(H,H) = 9.0 Hz, 2H; H^{11}, H^{13}), 4.27 (s, 3H; NCH_3), 3.40 (t, ^3J(H,H) = 7.8 Hz, 4H; NCH_2), 1.61 (m, 4H; -CH_2-), 1.43 (m, 4H; CH_2), 1.01 (t, ^3J(H,H) = 7.3 Hz, 6H; CH_3): elemental analysis (%) calcd (found): C 34.92 (34.88), H 3.78 (3.81), N 3.39 (3.32).

Acknowledgements

This work was supported by the Ministero dell'Istruzione, dell'Università e della Ricerca (research project FIRB, year 2001, title: "Nano-Organization of Hybrid Organo-Inorganic Molecules with Magnetic and Non Linear Optical Properties" and project PRIN, year 2007, title: "Nuove strategie per il controllo di reazioni metallo assistite: interazioni non convenzionali di frammenti molecolari"). We deeply thank Dr. Stefania Righetto for help in EFISH measurements.

Keywords: aggregation · cations · chromophores · ion pairs · nonlinear optics

[1] a) *Nonlinear Optical Properties of Organic Molecules and Crystals, Vol. 1* (Eds.: D. S. Chemla, J. Zyss), Academic Press, Orlando, **1987**; b) *Molecular Nonlinear Optics: Materials, Physics and Devices* (Ed.: J. Zyss), Academic Press, Boston, **1994**; c) N. J. Long, *Angew. Chem.* **1995**, *107*, 37 – 56; *Angew. Chem. Int. Ed. Engl.* **1995**, *34*, 21 – 38; d) H. S. Nalwa, S. Miyata, *Nonlinear Optics of Organic Molecules and Polymers*, CRC Press, Boca Raton, **1996**; e) B. J. Coe, *Comprehensive Coordination Chemistry II, Vol. 9* (Eds: J. A. McCleverty, T. J. Meyer), Elsevier Pergamon, Oxford, **2004**, pp. 621 – 687.

[2] a) B. J. Coe, J. A. Harris, I. Asselberghs, K. Clays, G. Olbrechts, A. Persoons, J. T. Hupp, R. C. Johnson, S. J. Coles, M. B. Hursthouse, K. Nakatani, *Adv. Funct. Mater.* **2002**, *12*, 110 – 116; b) B. J. Coe, J. A. Harris, I. Asselberghs, K. Wostyn, K. Clays, A. Persoons, B. S. Brunschwig, S. J. Coles, T. Gelbrich, M. E. Light, M. B. Hursthouse, K. Nakatani, *Adv. Funct. Mater.* **2003**, *13*, 347 – 357 and references therein.

[3] G. R. Meredith, *Nonlinear Optical Properties of Organic and Polymeric Materials* (Ed.: J. D. Williams), ACS Symposium Series, American Chemical Society, Washington, **1983**, *233*, 27 – 56.

[4] a) S. R. Marder, J. W. Perry, W. P. Schaefer, *Science* **1989**, *245*, 626 – 628; b) S. R. Marder, J. W. Perry, C. P. Yakymyshyn, *Chem. Mater.* **1994**, *6*, 1137 – 1147.

[5] S. Di Bella, I. Fragalà, M. A. Ratner, T. J. Marks, *Chem. Mater.* **1995**, *7*, 400 – 404.

[6] a) B. F. Levine, C. G. Bethea, *Appl. Phys. Lett.* **1974**, *24*, 445–447; b) K. D. Singer, A. F. Garito, *J. Chem. Phys.* **1981**, *75*, 3572–3580; c) I. Ledoux, J. Zyss, *Chem. Phys.* **1982**, *73*, 203–213.

[7] V. Alain, M. Blanchard-Desce, I. Ledoux-Rak, J. Zyss, *Chem. Commun.* **2000**, 353–354.

[8] a) R. W. Terhune, P. D. Maker, C. M. Savage, *Phys. Rev. Lett.* **1965**, *14*, 681–684; b) K. Clays, A. Persoons, *Phys. Rev. Lett.* **1991**, *66*, 2980–2983; c) K. Clays, A. Persoons, *Rev. Sci. Instrum.* **1992**, *63*, 3285–3289; d) K. Clays, A. Persoons, L. De Maeyer, *Modern Nonlinear Optics* (Eds.: M. Evans, S. Kielich), Wiley, New York, **1994**; e) E. Hendrickx, K. Clays, A. Persoons, *Acc. Chem. Res.* **1998**, *31*, 675–683.

[9] a) M. C. Flipse, R. De Jonge, R. H. Woundenberg, A. W. Marsman, A. van Walree, L. W. Jenneskens, *Chem. Phys. Lett.* **1995**, *245*, 297–303; b) I. D. Morrison, R. G. Denning, W. M. Laidlaw, M. A. Stammers, *Rev. Sci. Instrum.* **1996**, *67*, 1445–1453; c) S. Stadler, G. Bourhill, C. Bräuchle, *J. Phys. Chem.* **1996**, *100*, 6927–6934.

[10] F. Tessore, D. Roberto, R. Ugo, P. Mussini, S. Quici, I. Ledoux-Rak, J. Zyss, *Angew. Chem.* **2003**, *115*, 472–475, *Angew. Chem. Int. Ed.* **2003**, *42*, 456–459.

[11] F. Tessore, D. Locatelli, S. Righetto, D. Roberto, R. Ugo, P. Mussini, *Inorg. Chem.* **2005**, *44*, 2437–2442.

[12] A. Macchioni, G. Ciancaleoni, C. Zuccaccia, D. Zuccaccia, *Chem. Soc. Rev.* **2008**, *37*, 479–489 and references therein.

[13] a) D. Roberto, E. Cariati, R. Psaro, R. Ugo, *Organometallics* **1994**, *13*, 4227; b) J. Herde, J. C. Lambert, C. V. Senoff, *Inorg. Synth.* **1974**, *15*, 18–20.

[14] a) E. A. Guggenheim, *Trans. Faraday Soc.* **1949**, *45*, 714–720; b) W. Smith, *Electric Dipole Moments*, Butterworth Scientific Publications, London, **1965**; c) B. H. Thompson, *J. Chem. Educ.* **1966**, *43*, 66–73.

[15] K. M. Begum, E. Grunwald, *J. Am. Chem. Soc.* **1990**, *112*, 5104–5110, and references therein.

[16] E. Grunwald, C. K. Pan, *J. Phys. Chem.* **1976**, *80*, 2929–2931, and references therein.

[17] a) E. Lucenti, E. Cariati, C. Dragonetti, L. Manassero. F. Tessore, *Organometallics* **2004**, *23*, 687–692; b) D. Roberto, R. Ugo, S. Bruni, E. Cariati, F. Cariati, P. C. Fantucci, I. Invernizzi, S. Quici, I. Ledoux, J. Zyss, *Organometallics* **2000**, *19*, 1775–1788.

[18] B. J. Coe, D. Beljonne, H. Vogel, J. Garín, J. Orduna, *J. Phys. Chem. A* **2005**, *109*, 10052–10057.

[19] a) D. R. Kanis, P. G. Lacroix, M. A. Ratner, T. J. Marks, *J. Am. Chem. Soc.* **1994**, *116*, 10089–10102; b) M. J. G. Lesley, A. Woodward, N. J. Taylor, T. B. Marder, I. Cazenobe, I. Ledoux, J. Zyss, A. Thornton, D. W. Bruce, A. K. Kakkar, *Chem. Mater.* **1998**, *10*, 1355–1365.

[20] D. G. Whitten, *Acc. Chem. Res.* **1993**, *26*, 502–509.

[21] W. J. Oldham, Y. J. Miao, R. I. Lachicotte, G. C. Bazan, *J. Am. Chem. Soc.* **1998**, *120*, 419–420.

[22] B. J. Orr, J. F. Ward, *Mol. Phys.* **1971**, *20*, 513–526.

[23] The high $\mu\beta_{1.91}$ values observed on dilution could be underestimated, because migration of the ions may decrease the electric field and therefore the alignment of the NLO chromophores in solution.

[24] C. A. Kraus, W. C. Bray, *J. Am. Chem. Soc.* **1913**, *35*, 1315–1434.

[25] a) R. M. Fuoss, C. A. Kraus, *J. Am. Chem. Soc.* **1933**, *55*, 21–36; b) R. M. Fuoss, C. A. Kraus, *J. Am. Chem. Soc.* **1933**, *55*, 476–488; c) R. M. Fuoss, C. A. Kraus, *J. Am. Chem. Soc.* **1933**, *55*, 10191028.

[26] Theoretical expressions of *f* have been obtained for prolate or oblate ellipsoids by Perrin (F. Perrin, *J. Phys. Radium* **1936**, *7*, 1–11). The corresponding expressions for ellipsoids having three unequal axes was obtained by Elworthy (P. H. Elworthy, *J. Chem. Soc.* **1962**, 3718–3723).

[27] The ^{127}I isotope is quadrupolar ($I = 5/2$) and consequently difficult to investigate by means of diffusion experiments.

[28] Both orientations are found, for example, in the solid state of the related 4′-dimethylamino-*N*-methyl-4-stilbazolium *p*-toluensulfonate monohydrate salt: G. L. Bryant, Jr., C. P. Yakymyshyn, K. R. Stewart, *Acta Crystallogr. Sect. C* **1993**, *49*, 350–351.

[29] F. Nunzi, S. Fantacci, F. De Angelis, A. Sgamellotti, E. Cariati, R. Ugo, P. Macchi, *J. Phys. Chem. C* **2008**, *112*, 1213–1226.

[30] Other arrangements have been proposed for tetrasubstituted ammonium salts. See, for example: L. Comeford, E. Grunwald, K. M. Begum, J. Pradhan, *J. Phys. Chem.* **1990**, *94*, 2714–2716.

[31] L. A. Dominey, L. Comeford, S. J. H. Chen, E. Grunwald, *J. Phys. Chem.* **1987**, *91*, 2211–2216, and references therein.

[32] A. Macchioni, *Eur. J. Inorg. Chem.* **2003**, 195–205 and references therein.

[33] Y. Wang. D. L. Frattarelli, A. Facchetti, E. Cariati, E. Tordin, R. Ugo, C. Zuccaccia, A. Macchioni, S. L. Wegener, C. L. Stern, M. A. Ratner, T. J. Marks, *J. Phys. Chem. C* **2008**, *112*, 8005–8015.

[34] R. B. Martin, *Chem. Rev.* **1996**, *96*, 3043–3064, and references therein.

[35] G. Ciancaleoni, I. Di Maio, D. Zuccaccia, A. Macchioni, *Organometallics* **2007**, *26*, 489–496.

[36] M. Valentini, H. Rüegger, P. S. Pregosin, *Helv. Chim. Acta* **2001**, *84*, 2833, and references therein.

[37] R. Mills, *J. Phys. Chem.* **1973**, *77*, 685–688.

Received: September 2, 2009